AIP Journal of Applied Physics

Perfect spin-valley filter controlled by electric field in ferromagnetic silicene

Bumned Soodchomshom

Citation: Journal of Applied Physics **115**, 023706 (2014); doi: 10.1063/1.4861644
View online: http://dx.doi.org/10.1063/1.4861644
View Table of Contents: http://scitation.aip.org/content/aip/journal/jap/115/2?ver=pdfcov
Published by the AIP Publishing

JOURNAL OF APPLIED PHYSICS **115**, 023706 (2014)

Perfect spin-valley filter controlled by electric field in ferromagnetic silicene

Bumned Soodchomshom[a)]
Department of Physics, Faculty of Science, Kasetsart University, Bangkok 10900, Thailand

(Received 14 November 2013; accepted 23 December 2013; published online 10 January 2014)

The spin-valley currents in silicene-based normal/sublattice-dependent ferromagnetic/normal junction are investigated. Unlike that in graphene, the pseudo Dirac mass in silicene is generated by spin-orbit interaction and tunable by applying electric or exchange fields into it. This is due to silicon-based honeycomb lattice having buckled structure. As a result, it is found that the junction leads to currents perfectly split into four groups, spin up (down) in k- and k′-valleys, when applying different values of the electric field, considered as a perfect spin-valley polarization (PSVP) for electronic application. The PSVP is due to the interplay of spin-valley-dependent Dirac mass and chemical potential in the barrier. The PSVP also occurs only for the energy comparable to the spin-orbit energy gap. This work reveals potential of silicene for spinvalleytronics applications. © *2014 AIP Publishing LLC*. [http://dx.doi.org/10.1063/1.4861644]

I. INTRODUCTION

After the discovery of graphene,[1] a mono layer of graphite, several of its intriguing properties led graphene to become a promising material for the fields of nanoelectronics[2] and high energy-like physics.[3] Graphene is formed by the carbon atoms arranged planar honeycomb lattice due to the sp^2-hybridization. Electrons in graphene behave like two-dimensional Dirac fermions, where the wave functions of electron in A- and B-sublattices play the role of wave states of electron with pseudo spin-up and spin-down, respectively. Electrons in graphene have two valley degrees of freedom, k− and k′−valleys. The presence of the valley degrees of freedom in graphene leads to the so-called "valleytronics," since valley currents can be controllable.[4,5] Recently, silicene, a new honeycomb-like atomic structure formed by the silicon atoms, which has electronic band structure akin to graphene, has been first synthesized.[6,7] The presence of strong spin-orbit interaction and buckled structure in silicene unlike that in graphene leads to several interesting electronic properties such as Dirac mass controlled by electric field,[8,9] and its band structure is (real) spin-valley-dependent,[10] applicable for silicene-based spin-valleytronics. Graphene lacks these properties because its honeycomb structure is planar and has very small spin-orbit interaction.[11] Hence, the coupling between spin and valleys in graphene is very weak. There has been considerable attention drawn to study electronic property of silicene[12–15] and its potential applications.[16–19]

Recently, the transport property in silicene has been investigated.[17–19] Charge transport in pn and npn junctions[17] was found to be almost quantized to be 0, 1, and 2. The spin-valley polarization in magneto-optical response of silicene has been investigated.[19] Tabert and Nicol[19] showed that distinct spin and valley currents can be seen in the longitudinal magneto optical conductivity which is experimental accessible. Control of spin and valley currents was studied in a proximity-induced ferromagnetic silicene NM/FM/NM junction,[18] where NM and FM are normal and ferromagnetic silicene layers, respectively. Pure-spin and pure-valley currents were found to be tunable by electric and exchange fields in the FM-layer. The study of spin-valley transport in Ref. 18 has taken into account only the condition of which the ferromagnetism in A- and B-sublattices in the FM-layer is assumed to have the same exchange field strength. In the case of Ref. 18, there is no spin-dependent magnetic energy gap to generate spin-valley dependent Dirac mass in the FM-region. In graphene, the valley-polarization occurs when graphene is under both strain and magnetic vector potential.[20,21] The spin-valley transport in graphene may take place when the Zeeman filed is applied into the junction.[5,22] In silicene junction, the strain and vector potential are not required to generate spin-valley polarization.[18]

In this paper, the spin-valley conductances in silicene-based normal (NM)/sublattice-dependent ferromagnetic (SFM)/normal (NM) junction are investigated. We study the SFM silicene in the present work, based on the tight-binding Hamiltonian recently modeled in Ref. 10. The exchange fields in the A- and B-sublattices are assumed to be different, leading to the energy gap induced by the exchange field.[10] We will show that the distinct spin and valley currents, a perfect spin-valley polarization (PSVP), would take place due to the interplay of chemical potential and the effect of sublattice-dependent ferromagnetism in silicene at the barrier. The PSVP can also be controlled by the external electric field applied into the barrier.

II. MODEL AND HAMILTONIAN

The model of silicene-based NM/SFM/NM junction is depicted in Fig. 1(a). The silicene-based magnetic barrier or SFM-layer with thickness L is induced into ferromagnetism for the A- and B-sublattices by the different magnetic insulators. The exchange energies induced by the top and

[a)]Author to whom correspondence should be addressed. Electronic addresses: Bumned@hotmail.com and fscibns@ku.ac.th

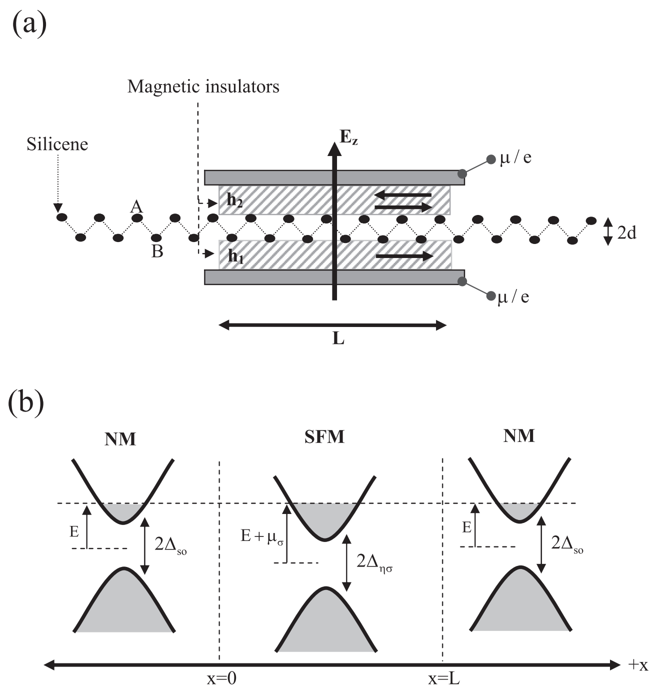

FIG. 1. Model of (a) NM/SFM/NM junction and (b) the Fermi level of electron in each region. The exchange fields are induced into A- and B-sublattices with different values h_1 and h_2, respectively.

the bottom magnetic insulators into A- and B-sublattices are h_1 and h_2, respectively. The chemical potential μ is induced by the top and the bottom gates with the same potential μ/e. The silicene sheet has a perpendicular distance between A- and B-sublattices of $2d = 0.43$ Å (Ref. 10). The electric field E_z perpendicular to silicene sheet is applied into the barrier-region and may be controllable. In this section, we first consider the non-interacting electrons in silicene (NM-layer) described based on Kane-Mele model[23]

$$\mathrm{H}_{NM} = -\mathrm{t}\sum_{\langle \mathrm{i,j}\rangle\alpha} \mathrm{c}^{\dagger}_{\mathrm{i}\alpha}\mathrm{c}_{\mathrm{j}\alpha} + \mathrm{i}\frac{\Delta_{\mathrm{so}}}{3\sqrt{3}}\sum_{\langle\langle \mathrm{i,j}\rangle\rangle\alpha,\beta} \lambda_{\mathrm{ij}}\mathrm{c}^{\dagger}_{\mathrm{i}\alpha}\sigma^{z}_{\alpha\beta}\mathrm{c}_{\mathrm{j}\beta} - \mathrm{i}\frac{2}{3}\Delta_R\sum_{\langle\langle \mathrm{i,j}\rangle\rangle\alpha,\beta}\kappa_{\mathrm{i}}\mathrm{c}^{\dagger}_{\mathrm{i}\alpha}(\vec{\sigma}\times\hat{\mathrm{d}}_{\mathrm{ij}})^{z}_{\alpha\beta}\mathrm{c}_{\mathrm{j}\beta}, \tag{1}$$

where $\mathrm{c}^{\dagger}_{i\alpha(\beta)}$ is creation operator of electron with spin polarization α (β) at site i and the notation $\langle \mathrm{i,j}\rangle$ ($\langle\langle \mathrm{i,j}\rangle\rangle$) are associated with summation over all the nearest (next-nearest) neighbor hoping sites. The hoping energy of electron transferring between the nearest neighbor atoms for silicene is $\mathrm{t} = 1.6$ eV. The effective spin-orbit interaction is $\Delta_{\mathrm{so}} = 3.9$ meV,[12] where $\lambda_{\mathrm{ij}} = 1(-1)$ if the next-nearest-neighbor hoping is counterclockwise (clockwise) with respect to the positive z-axis, direction perpendicular to silicene plane. The Rashba interaction is $\Delta_{\mathrm{R}} = 0.7$ meV,[10] where $\kappa_{\mathrm{i}} = 1(-1)$ stands for A-(B-) sublattice. The notation $\hat{\mathrm{d}}_{\mathrm{ij}} = \vec{\mathrm{d}}_{\mathrm{ij}}/|\vec{\mathrm{d}}_{\mathrm{ij}}|$ represents the vector connecting two sites i and j for the same sublattice. The Pauli spin-operators used to represent **real** and **sublattice** spins are $\vec{\sigma} = \langle\sigma^{x},\sigma^{y},\sigma^{z}\rangle$ and $\vec{\tau} = \langle\tau^{x},\tau^{y},\tau^{z}\rangle$, respectively. In the SFM-layer, based on Ref. 10, silicene under the influence of the gate potential μ/e, electric field E_{z}, and the exchange energy $\mathrm{M}_{\mathrm{i}} = \mathrm{h}_1(\mathrm{h}_2)$ for A- (B-) sublattice may be described by using the tight-binding model of the form

$$H_{SFM} = H_{NM} - \mu\sum_{i,\alpha} c^{\dagger}_{i\alpha}c_{i\alpha} - edE_Z\sum_{i,\alpha}\kappa_i c^{\dagger}_{i\alpha}c_{i\alpha} - \sum_{i,\alpha} M_i c^{\dagger}_{i\alpha}\sigma^{z}_{\alpha\alpha}c_{i\alpha}. \tag{2}$$

The tight-binding Hamiltonians in Eqs. (1) and (2) may yield the low-energy effective Hamiltonians used to describe the motion of electron in A-and B-sublattices, respectively, with spin $\sigma = \uparrow,\downarrow$ in the NM- and SFM-regions. At the low energy, the effect of Rashba interaction is very small comparing with the other terms.[10,18] The wave equation in the $k(k')$ valleys, denoted by $\eta = 1(-1)$, with excited energy E, is therefore obtained by

$$\mathrm{H}_{\eta\sigma}\psi_{\eta\sigma} = \mathrm{E}\psi_{\eta\sigma}, \tag{3}$$

where

$$\mathrm{H}_{\eta\sigma} = \mathrm{v_F}(\hat{\mathrm{p}}_{\mathrm{x}}\tau^{\mathrm{x}} - \eta\hat{\mathrm{p}}_{\mathrm{y}}\tau^{\mathrm{y}}) - \Delta_{\eta\sigma}\tau^{\mathrm{z}} - \mu_{\sigma},$$

with $\hat{\mathrm{p}}_{\mathrm{x}} = -\mathrm{i}\hbar\frac{\partial}{\partial \mathrm{x}}$ and $\hat{\mathrm{p}}_{\mathrm{y}} = -\mathrm{i}\hbar\frac{\partial}{\partial \mathrm{y}}$.

The Hamiltonian in Eq. (3) would act on the pseudo spin-valley dependent spinor field, $\psi_{\eta\sigma} = \begin{pmatrix}\psi_{\mathrm{A}\eta\sigma}\\ \psi_{\mathrm{B}\eta\sigma}\end{pmatrix}$, where $\psi_{\mathrm{A}\eta\sigma}$ and $\psi_{\mathrm{B}\eta\sigma}$ are the wave functions of electrons with spin $\sigma = \uparrow,\downarrow$ and k, k′-valleys in A- and B-sublattices, respectively. In silicene, the Fermi velocity found near the Dirac point is about $\mathrm{v_F} \cong 5.5\times10^{5}$ m/s.[12] The spin-valley dependent energy gap is given by $\Delta_{\eta\sigma} = \eta\sigma\Delta_{\mathrm{so}} - \Delta_{\mathrm{E}} + \sigma\Delta_{\mathrm{M}}$, which is associated with the spin-orbit interaction (Δ_{so}), the electric field ($\Delta_{\mathrm{E}} = \mathrm{edE_Z}$), and the lattice-dependent exchange field ($\Delta_{\mathrm{M}} = \frac{\mathrm{h_1}-\mathrm{h_2}}{2}$). The chemical potential in the barrier is also spin-dependent related to the exchange field. We therefore define $\mu_{\sigma} = \mu + \sigma\mathrm{u_M}$ as the spin-dependent chemical potential in the barrier, where $\mathrm{u_M} = \left(\frac{\mathrm{h_1}+\mathrm{h_2}}{2}\right)$. We note that the Hamiltonian in Eq. (3) can be reduced into the same form as found in Ref. 18 when there are no gate-induced chemical potential ($\mu \to 0$) and no lattice-dependent exchange field ($\Delta_{\mathrm{M}} \to 0$ and $\mathrm{u_M} \neq 0$) in the barrier.

The Hamiltonian in Eq. (3) yields the Eigen value as of the form

$$\mathrm{E} = +(-)\sqrt{(\mathrm{v_F p})^2 + \Delta^2_{\eta\sigma}} - \mu_{\sigma}. \tag{4}$$

The sign $+(-)$ stands for band energy of electron(hole). When we take the relativistic-mass relation of the form mass $= \Delta_{\eta\sigma}/\mathrm{v}^2_{\mathrm{F}}$, electrons in silicene can be considered as relativistic particles with spin-valley-dependent mass. The Dirac mass of electrons in silicene is tunable by the electric and the exchange fields, unlike that in graphene. Masses of electrons in silicene are spin-valley dependent, i.e.,

$$\Delta_{k\uparrow} = \Delta_{so} - \Delta_E + \Delta_M, \quad \Delta_{k\downarrow} = -(\Delta_{so} + \Delta_E + \Delta_M),$$
$$\Delta_{k'\uparrow} = -\Delta_{so} - \Delta_E + \Delta_M \text{ and } \Delta_{k'\downarrow} = \Delta_{so} - \Delta_E - \Delta_M. \quad (5)$$

The magnitudes of masses in each valley and spin can be tunable differently $\Delta_{k\uparrow} \neq \Delta_{k'\uparrow} \neq \Delta_{k\downarrow} \neq \Delta_{k'\uparrow}$. If there is no exchange-field-induced energy gap $\Delta_M \to 0$,[18] we will see that $\Delta_{k\uparrow} = \Delta_{k'\downarrow}$ and $\Delta_{k\downarrow} = \Delta_{k'\uparrow}$. In Sec. III, we will show the influence of multi-mass-carrier properties on the electronic transport. The perfect spin-valley polarization controlled by electric field will be predicted.

III. SCATTERING PROCESS

The spin-valley tunneling process in our model as seen in Fig. 1(a) is investigated in this section. We adopt the Hamiltonian in Eq. (3) to describe the motion of electrons in the system. The spin-valley currents are flowing along the x-direction. The Fermi level of electron in each region is depicted in Fig. 1(b). The model leads to the Fermi level as of the form $\mu_\sigma(0 \le x \le L) = \mu + \sigma(h_1 + h_2)/2$. The electric-field-induced energy and the exchange-field-induced energy can be defined, respectively, as $\Delta_E(0 \le x \le L) = edE_Z$ and $\Delta_M(0 \le x \le L) = \frac{h_1 - h_2}{2}$. In the NM regions, defined in $x \le 0$ and $x \ge L$, we have $\mu_\sigma = \Delta_M = \Delta_E = 0$. Then, the wave function in the left-NM, SFM, and the right-NM are, respectively, given as

$$\psi_{NM1} = \left[\begin{pmatrix} 1 \\ A_{\eta\sigma}e^{-i\eta\theta} \end{pmatrix} e^{ik_x x} + r_{\eta\sigma}\begin{pmatrix} 1 \\ -A_{\eta\sigma}e^{i\eta\theta} \end{pmatrix} e^{-ik_x x}\right] e^{ik_{//}y},$$
$$\psi_{SFM} = \left[a_{\eta\sigma}\begin{pmatrix} 1 \\ B_{\eta\sigma}e^{-i\eta\beta} \end{pmatrix} e^{iq_x x} + b_{\eta\sigma}\begin{pmatrix} 1 \\ -B_{\eta\sigma}e^{i\eta\beta} \end{pmatrix} e^{-iq_x x}\right] e^{ik_{//}y},$$

and

$$\psi_{NM2} = \left[t_{\eta\sigma}\begin{pmatrix} 1 \\ A_{\eta\sigma}e^{-i\eta\theta} \end{pmatrix} e^{ik_x x}\right] e^{ik_{//}y},$$

where

$$A_{\eta\sigma} = \frac{E + \eta\sigma\Delta_{so}}{\sqrt{E^2 - \Delta_{so}^2}}, \quad B_{\eta\sigma} = \frac{E + \mu_\sigma + \Delta_{\eta\sigma}}{\sqrt{(E + \mu_\sigma)^2 - \Delta_{\eta\sigma}^2}} \text{ with}$$
$$\mu_\sigma = \mu + \sigma\left(\frac{h_1 + h_2}{2}\right) \quad \text{and}$$
$$\Delta_{\eta\sigma} = \eta\sigma\Delta_{so} - edE_z + \sigma\left(\frac{h_1 - h_2}{2}\right). \quad (6)$$

The wave vectors in the x-direction of electron in NM and SFM region are given by $k_x = \sqrt{E^2 - \Delta_{so}^2}\cos\theta/\hbar v_F$ and $q_x = \sqrt{(E + \mu_\sigma)^2 - \Delta_{\eta\sigma}^2}\cos\beta/\hbar v_F$, respectively. The incident angle "β" in the SFM barrier can be calculated via the conservation component in the y-direction as given by $k_{/\!/} = \sqrt{E^2 - \Delta_{so}^2}\sin\theta/\hbar v_F = \sqrt{(E + \mu_\sigma)^2 - \Delta_{\eta\sigma}^2}\sin\beta/\hbar v_F$, where "$\theta$" is the incident angle in the NM-regions. The coefficients $r_{\eta\sigma}$, $a_{\eta\sigma}$, $b_{\eta\sigma}$, and $t_{\eta\sigma}$ can be calculated through the boundary conditions at the interfaces $\psi_{NM1}(0) = \psi_{SFM}(0)$ and $\psi_{SFM}(L) = \psi_{NM2}(L)$. Here, $r_{\eta\sigma}$ and $t_{\eta\sigma}$ are called the reflection and transmission coefficients, respectively. By matching the wave functions and the boundary conditions, the spin-valley-dependent transmission coefficient is obtained as

$$t_{\eta\sigma} = \frac{A_{\eta\sigma}B_{\eta\sigma}e^{-iL(k_x - q_x)}(1 + e^{2i\eta\beta})(1 + e^{2i\eta\theta})}{A_{\eta\sigma}B_{\eta\sigma}e^{2i\eta(\beta+\theta)} - (A_{\eta\sigma}^2 + B_{\eta\sigma}^2)e^{i\eta(\beta+\theta)}(e^{2iLq_x} - 1) + A_{\eta\sigma}B_{\eta\sigma}(1 + e^{2i(Lq_x + \eta\beta)} + e^{2i(Lq_x + \eta\theta)})}. \quad (7)$$

The transmission probability amplitude "$T_{\eta\sigma}$" is calculated via the formula $T_{\eta\sigma} = J_t/J_{in}$, where J_t and J_{in} are the current densities of the transmitted electron and the injected electron, respectively. In our work, the current density operator in the x-direction is found to be $\hat{J}_x = v_F\tau^x$. Hence, the transmission probability amplitude may be obtained as $T_{\eta\sigma} = J_t/J_{in} = (\psi_t^*)^T\hat{J}_x\psi_t/(\psi_{in}^*)^T\hat{J}_x\psi_{in} = |t_{\eta\sigma}|^2$, where ψ_t and ψ_{in} are the wave functions of the transmitted electron and the injected electron, respectively.

IV. SPIN-VALLEY CONDUCTANCE FORMULAE

The spin-valley conductance at the zero temperature in the ballistic regime may be calculated using the standard Landauer's formalism[24] by integrating overall the incident angles

$$G_{\eta\sigma} = \frac{e^2}{h}N(E)|t_{\eta\sigma}|^2 = \frac{e^2}{h}\sum_{\vec{k}}\delta(E - E(k))\frac{\pi\hbar}{D}\left|\frac{1}{\hbar}\partial E/\partial k_x\right|T_{\eta\sigma},$$
$$G_{\eta\sigma} = G_0\frac{\sqrt{E^2 - \Delta_{so}^2}}{|E|}\int_{-\pi/2}^{\pi/2}\frac{1}{8}d\theta\cos(\theta)T_{\eta\sigma}, \quad (8)$$

where $\vec{k}$ is wave vector of electron in the NM-layers and $\delta(E)$ is a Dirac-delta function. $G_0 = \frac{4e^2}{h}N_0(E)$ is defined as a unit conductance, where $N_0(E) = \frac{W}{\pi\hbar v_F}|E|$ is the density of state in transport channel for silicene with no spin-orbit-interaction and "h" is the Planck's constant. W and D are width and length of silicene sheet, respectively. We note that the density of state in transport channel for normal silicene junction is $N(E) = \frac{W}{\pi\hbar v_F}\sqrt{E^2 - \Delta_{so}^2}$. The total conductance

G_T of the junction is calculated using the summation of all spin-valley conductances

$$G_T = G_{k\uparrow} + G_{k\downarrow} + G_{k'\uparrow} + G_{k'\downarrow}, \quad \text{where} \quad G_{k\uparrow} = G_{\eta=1,\sigma=\uparrow}, \quad G_{k\downarrow} = G_{\eta=1,\sigma=\downarrow}, \quad G_{k'\uparrow} = G_{\eta=-1,\sigma=\uparrow}, \quad \text{and} \quad G_{k'\downarrow} = G_{\eta=-1,\sigma=\downarrow}. \tag{9}$$

The spin-valley conductance given in Eq. (8) vanishes, when the excited energy E is smaller than Δ_{so}, saying that silicene becomes insulating state in the NM-layers in this regime.

V. RESULT AND DISCUSSION

In numerical result, the electric-field-induced band gap in silicene is studied in the range that should be accessible.[9] The magnetic insulator EuO may give rise to proximity-induced exchange energy of 5 meV, proposed previously for inducing ferromagnetism in graphene.[25] We take the spin-orbit interaction $\Delta_{so} = 3.9$ meV for the calculation.[12] The parallel (P) and anti-parallel (AP) junctions are defined using the conditions of $h_1 = h_2 = 5$ meV and $h_1 = -h_2 = 5$ meV, respectively. The conductance at the excited energy approaching the spin-orbit energy gap $E \rightarrow \Delta_{so}$ is focused, in order to show the strong Dirac mass effect. The plot of spin-valley conductances are normalized with G_0.

First, the spin-valley conductance as a function of E_z in the non-magnetic junction ($h_{1,2} = 0$) is studied for L = 25 nm. In Fig. 2(a), it is found that $G_{k\uparrow} = G_{k\downarrow} = G_{k'\uparrow} = G_{k'\downarrow}$ when we take $\mu = 0$. The maximum conductance is found at $E_z = 0$. Interestingly when we take $\mu = 5$ meV, the resonant conductance peak is split into two group $G_{k\uparrow} = G_{k'\downarrow}$ and $G_{k\downarrow} = G_{k'\uparrow}$, found at $edE_z \rightarrow -\mu$ and $edE_z \rightarrow +\mu$, respectively (see Fig. 2(b)). To recall Eq. (5), we will see that the electrons in the $k\uparrow$- and $k'\downarrow$-states may acquire the mass of $mass_{k\uparrow} = mass_{k'\downarrow} = (\Delta_{so} - edE_z)/v_F^2$, while the electrons in $k\downarrow$- and $k'\uparrow$-states may acquire the mass of $mass_{k\downarrow} = mass_{k'\uparrow} = -(\Delta_{so} + edE_z)/v_F^2$. These two-type Hamiltonians with different masses lead to the different transport property for $G_{k\uparrow} = G_{k'\downarrow}$ but not equal to $G_{k\downarrow} = G_{k'\uparrow}$. It is found that in the limit of $E/\Delta_{so} \rightarrow 1$, the external electric field yielding the maximum conductances like resonant-peaks for $G_{k\sigma}$, and $G_{k'\sigma}$ may be, respectively, obtained as

$$edE_z \rightarrow -u_M + \sigma\Delta_M - \sigma\mu + \sigma(E - \Delta_{so}), \quad \text{and} \quad edE_z \rightarrow u_M + \sigma\Delta_M + \sigma\mu - \sigma(E - \Delta_{so}). \tag{10}$$

This equation is calculated based on the condition of $\frac{\partial G_{\eta\sigma}}{\partial E_z} = 0$, which is the mathematical condition to give rise to the maximum values for $G_{\eta\sigma}$ under varying electric filed. In the next discussion, we will show that Eq. (10) plays necessary condition leading to PSVP in the silicene-based ferromagnetic junction. As we have seen, there are still no spin-valley polarizations for non-magnetic junction, although the chemical potential causes the two splitting conductances in Fig. 2(b).

In Fig. 3, the exchange field is applied into the barrier in order to study the spin-valley transport in the AP-junction. The exchange fields in A- and B- sublattices are induced to have opposite direction, giving rise to $\Delta_M = 5$ meV and $u_M = 0$. As a result in Fig. 3(a), for $\mu = 0$, the very strong spin polarization occurs and it is controllable by E_z. The spin polarization is due to the presence of Δ_M. However, this case does not lead to the valley polarization. Interestingly, the

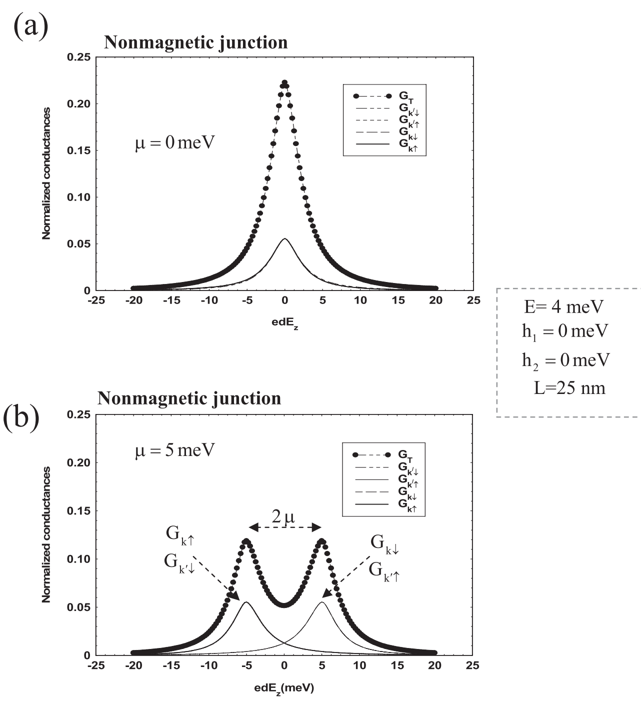

FIG. 2. Plot of spin-valley conductances versus electric field E_z in the case of nonmagnetic barrier $h_1 = h_2 = 0$. There is no spin-valley polarized in the case of (a) $\mu = 0$ and (b) $\mu \neq 0$.

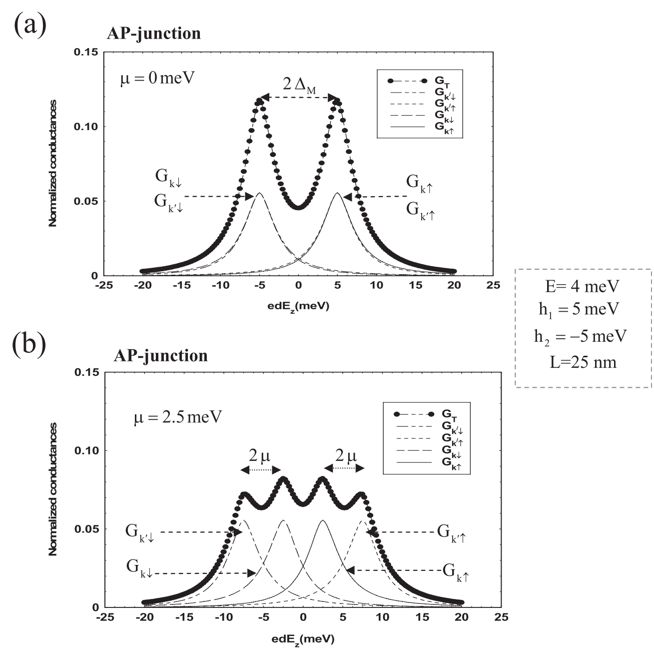

FIG. 3. Plot of spin-valley conductances in the AP-junction versus electric field E_z in the case of magnetic barrier $h_1 = -h_2 = 5\,meV$. There is solely spin polarization for (a) $\mu = 0$, while the spin-valley polarization occurs perfectly induced by the chemical potential for (b) $\mu \neq 0$.

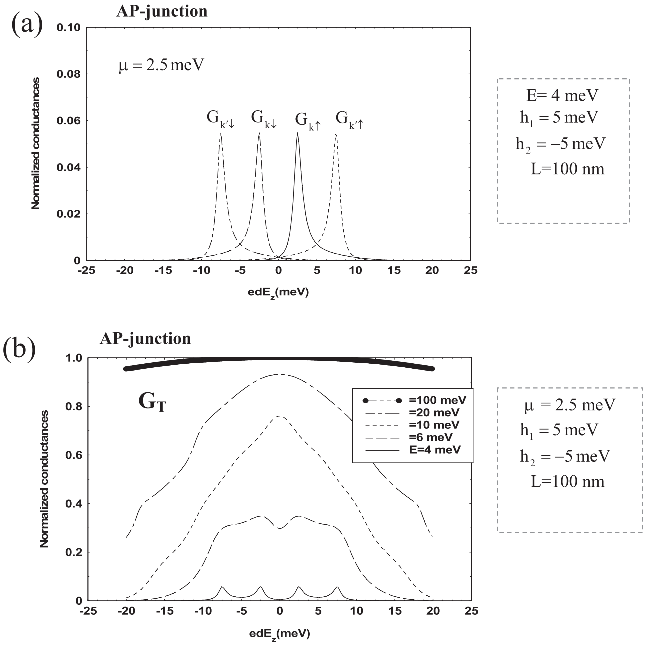

FIG. 4. Plot of spin-valley conductances in the AP-junction versus electric field E_z in the case of magnetic barrier $h_1 = -h_2 = 5\,\mathrm{meV}$. Perfect spin-valley splitting occurs for large $L = 100\,\mathrm{nm}$ (a). The spin-valley splitting disappears for large excited energy (b).

presence of very strong spin-valley polarization would take place when the chemical potential is applied $\mu \neq 0$ (see Fig. 3(b)). Predictable by Eq. (10), when the energy comparable to spin-orbit interaction $E/\Delta_{so} \to 1$, the conductance peaks of $G_{k\uparrow}$, $G_{k\downarrow}$, $G_{k'\uparrow}$, and $G_{k'\downarrow}$ do appear at $edE_z \to \Delta_M - \mu$, $-\Delta_M + \mu$, $\Delta_M + \mu$, and $-\Delta_M - \mu$, respectively. It can be concluded that the interplay of magnetic gap and the chemical potentials in the barrier would generate the PSVP in silicene. The resolution can be enhanced by increasing the thickness up to 100 nm (see Fig. 4(a)). The PSVP does not occur when the energy is very large $E \gg \Delta_{so}$ (see Fig. 4(b)).

The spin-valley transport in the P-junction is investigated in Figs. 5 and 6. The exchange fields in the A- and B- sublattices are induced to have the same direction, giving rise to $\Delta_M = 0$ and $u_M = 5\,\mathrm{meV}$. The chemical potential becomes spin-dependent $\mu_\sigma = \mu + \sigma u_M$. It is found that for $\mu = 0$, the valley polarization occurs solely (no spin polarization) as seen in Fig. 5(a). This is in contrast to that in the AP-junction which may give rise only to the spin polarization (see Fig. 3(a)). It is to say for $\mu = 0$, the P-junction can be used to control the valley polarization, while the AP-junction is used to control the spin polarization. We note that the very small off centre deviation between peaks around $edE_z = \pm u_M$ found in Fig. 5(a) can be described using Eq. (10). The maximum peaks of $G_{k\sigma}$ and $G_{k'\sigma}$ are found at $edE_z = -u_M + \sigma(E - \Delta_{so})$ and $edE_z = u_M - \sigma(E - \Delta_{so})$, respectively. Hence, the off centre deviation between peaks is still preserved because in the numerical result we have taken a small value of $E - \Delta_{so} = 0.1\,\mathrm{meV} \ll u_M \neq 0$. This small value has been neglected in the discussion. In the P-junction as seen in Fig. 5(b), spin-valley polarization is predicted for $\mu \neq 0$ similar to that in the AP-junction. The positions of conductance peaks of $G_{k\uparrow}$, $G_{k\downarrow}$, $G_{k'\uparrow}$, and $G_{k'\downarrow}$ are found at $edE_z \to -u_M - \mu$, $-u_M + \mu$, $u_M + \mu$, and $u_M - \mu$, respectively. It is also found that at $L = 100\,\mathrm{nm}$, the PSVP does not occur in case of the P-junction (see Fig. 6(a)) in

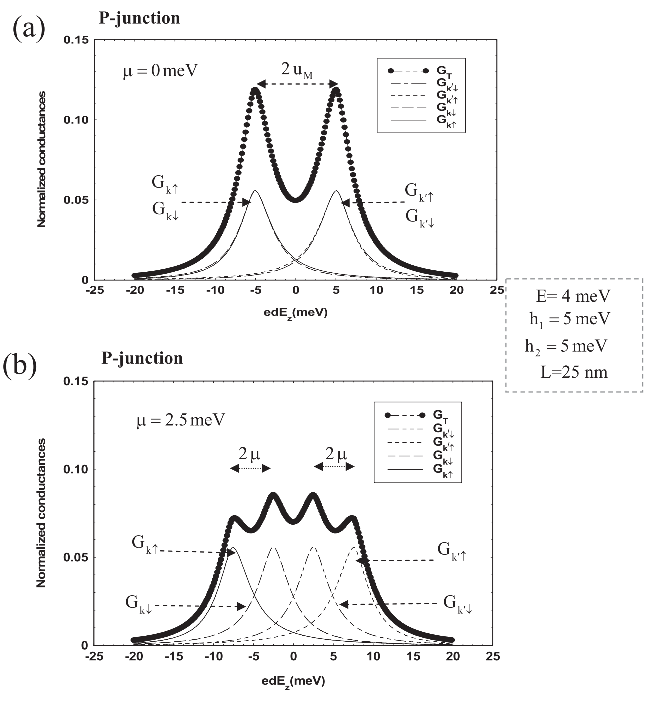

FIG. 5. Plot of spin-valley conductances in the P-junction versus electric field E_z in the case of magnetic barrier $h_1 = h_2 = 5\,\mathrm{meV}$. There is solely valley polarization for (a) $\mu = 0$, while the spin-valley polarization occurs quite perfectly induced by chemical potential for (b) $\mu \neq 0$.

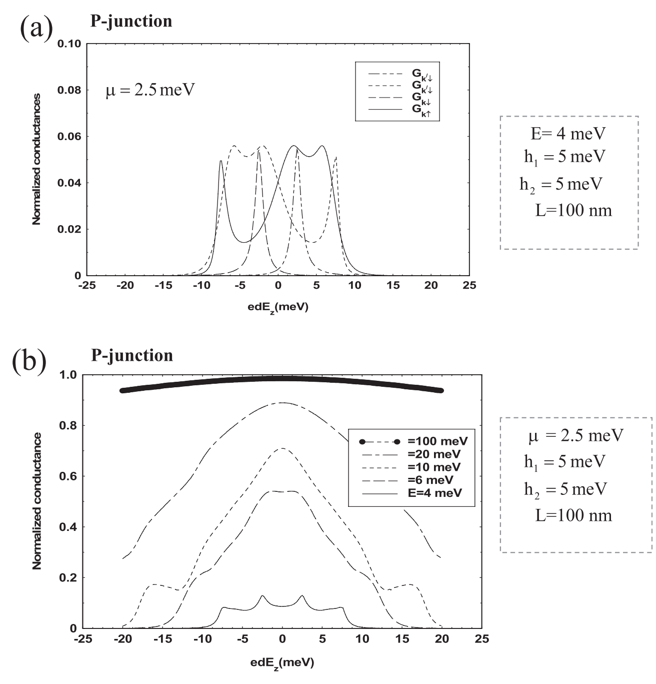

FIG. 6. Plot of spin-valley conductances in the P-junction versus electric field E_z in the case of magnetic barrier $h_1 = h_2 = 5\,\mathrm{meV}$. There is no perfect spin-valley splitting for large $L = 100\,\mathrm{nm}$ (a). The spin-valley splitting is absent for large excited energy (b).

contrast to the AP junction. Increasing E may also destroy the spin-valley polarization (see Fig. 6(b)) similar to that in the AP-junction. In Ref. 18, the spin-valley polarization does not report because there is no chemical potential $\mu = 0$ inside the barrier. The existence of the spin-valley polarization in a silicene-based NM/ferromagnetic/NM junction requires the condition of $\mu \neq 0$.

VI. SUMMARY AND CONCLUSION

We have investigated the spin-valley transport in a silicene-based normal/sublattice-dependent ferromagnetic/normal junction. The exchange field was assumed to be induced into A- and B-sublattices differently by magnetic insulators EuO,[25] leading to spin-dependent magnetic gap with 5 meV in the barrier. Remarkably, it was found that PSVP controlled by the external electric field occurs when the chemical potential and the exchange field are applied into the barrier. The energy of electron comparable to the spin-orbit interaction is also required for the existence of the PSVP. In the case of the absent chemical potential inside the barrier, the P junction can be used as an electronic junction to perfectly control the valley, while the AP junction is used to control the spin polarization. By means of proximity-induced ferromagnetism,[25] the PSVP predicted in our model may be testable. This work has revealed the potential of silicene for spin-valleytronics applications.

ACKNOWLEDGMENTS

This work was supported by Kasetsart University Research and Development Institute (KURDI).

[1] K. S. Novoselov *et al.*, Science **306**, 666 (2004).
[2] J. Basu *et al.*, Int. J. Smart Nano Mater. **1**, 201 (2010).
[3] Y. Wang *et al.*, Science **340**, 734 (2013).
[4] A. Rycerz *et al.*, Nature Phys. **3**, 172 (2007).
[5] B. Soodchomshom and P. Changarm, J. Supercond. Novel Magn. **24**, 1885 (2011).
[6] B. Lalmi *et al.*, Appl. Phys. Lett. **97**, 223109 (2010).
[7] P. D. Padova *et al.*, Appl. Phys. Lett. **96**, 261905 (2010).
[8] Z. Ni *et al.*, Nano Lett. **12**, 113 (2012).
[9] N. D. Drummond, V. Zolyomi, and V. I. Falko, Phys. Rev. B **85**, 075423 (2012).
[10] M. Ezawa, Phys. Rev. B **87**, 155415 (2013).
[11] A. H. Castro Neto and F. Guinea, Phys. Rev. Lett. **103**, 026804 (2009).
[12] C.-C. Liu *et al.*, Phys. Rev. Lett. **107**, 076802 (2011).
[13] M. Ezawa, Phys. Rev. Lett. **109**, 055502 (2012).
[14] L. Stille *et al.*, Phys. Rev. B **86**, 195405 (2012).
[15] F.-b. Zheng *et al.*, J. Mater. Chem. C **1**, 2735 (2013).
[16] M. Ezawa, Appl. Phys. Lett. **102**, 172103 (2013).
[17] A. Yamakage *et al.*, Phys. Rev. B **88**, 085322 (2013).
[18] T. Yokoyama, Phys. Rev. B **87**, 241409(R) (2013).
[19] C. J. Tabert and E. J. Nicol, Phys. Rev. Lett. **110**, 197402 (2013).
[20] F. Zhai and X. Zhao, Phys. Rev. B **82**, 115442 (2010).
[21] T. Fujita, M. B. A. Jalil, and S. G. Tan, Appl. Phys. Lett. **97**, 043508 (2010).
[22] Z. Niu, J. Appl. Phys. **111**, 103712 (2012).
[23] C. L. Kane and E. J. Mele, Phys. Rev. Lett. **95**, 226801 (2005).
[24] R. Landauer, IBM J. Res. Dev. **1**, 223 (1957).
[25] H. Haugen *et al.*, Phys. Rev. B **77**, 115406 (2008).